Controllable n-Type Doping on CVD-Grown Single- and Double-Layer Graphene Mixture

Wentao Xu, Lihua Wang, Yiwen Liu, Simil Thomas, Hong-Kyu Seo, Kwang-Ik Kim, Kwang S. Kim, and Tae-Woo Lee**

Graphene has possible applications in post-silicon nanoelectronics due to its high charge-carrier mobility, anomalous quantum Hall effect, and massless relativistic carriers.[1,2] Graphene usually works as a p-type material in air because of the presence of dangling bonds, adsorbed molecules, and residual polymers, although it is known theoretically to be ambipolar.[3–5] For complementary circuit applications, p-type graphene must be integrated with n-type graphene on a large scale.[6] Efforts have been made to investigate n-doping of single- or double-layer graphene.[7] However, graphene growth by using chemical vapor deposition (CVD) on copper often produces a mixture of single- and double-layer graphene instead of pure single- or double layers.[8] Although some initial attempts to n-dope CVD-grown graphene have been reported,[9,10] the properties of doped CVD-grown graphene thus cannot be simply explained by the predictions on n-doping of pure single- or double-layer graphene and the dependence of the overall properties of the doped-graphene mixture on single- and double layer fractions is still not understood.

n-type doping of graphene is often hindered by the energetic requirements for electron transfer from the dopant to the host.[11] Metallocenes with low ionization energy (IE) are relatively easy to use as efficient donors. Especially, decamethylcobaltocene (DMC) has a low IE of 3.3 eV, and is a powerful reductant that can n-dope a wide range of host materials including copper phthalocyanine (CuPc)[11] and pentacene[12] by coevaporation. The DMC molecule has abundant π-electrons that could strongly interact with and stably adhere to graphene lattices, and may thereby induce a distinct and stable doping effect. However, DMC doping of graphene has not yet been investigated experimentally. Experimental evidence is thus valuable to reveal possible doping effect of DMC on CVD-grown graphene.[13] In this work, we conducted a detailed investigation into the n-type doping effect of DMC on graphene grown using CVD. We also observed that the work function ϕ decreased quasilinearly as the logarithm of DMC solution concentration ([DMC]) increased; this relationship has obvious applications to tuning graphene properties for practical applications. We discuss the role of single- and double-layer fractions in determining the overall properties of n-doped CVD-grown graphene and explain the cause of the phenomenon theoretically. We also fabricated large-scale, well-aligned graphene nanoribbon field-effect transistor (GNRFET) arrays using electrohydrodynamic-printed-nanowire (e-NW) lithography, then n-type doped them and evaluated their electrical transport property and stability.

DMC was used to dope CVD-grown graphene that contains a mixture of single layers and double layers (**Figure 1**, and Supporting Information, SI-1). Raman spectroscopy is a powerful tool for studying the properties of graphene, such as the number of layers and the effects of doping.[14,15] The Raman spectra with typical G (1580–1590 cm^{-1}) and 2D bands (2690–2710 cm^{-1}) of the annealed and doped graphene is compared (**Figure 2**a). The spectra showed the typical shifts of G and 2D peaks of the graphene films after doping. As [DMC] increased, the G band shifted to a higher wavenumber by 5 cm^{-1}, and the 2D band shifted to a lower wavenumber by 6 cm^{-1}; these changes suggest that the annealed graphene was n-type doped[3] by DMC and that the doping effect could be enhanced by increasing [DMC]. This is similar to the effect of aromatic molecules with

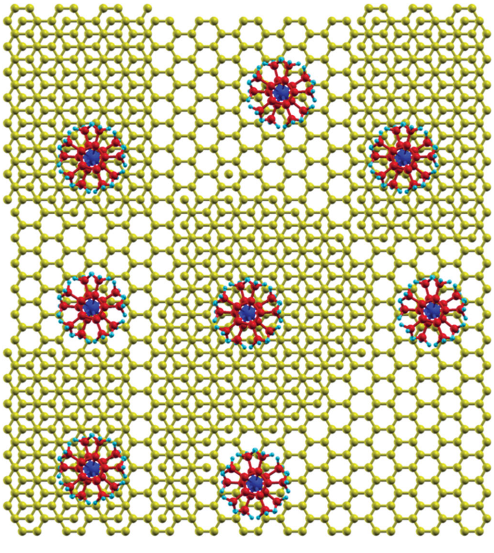

Figure 1. Schematic of the DMC molecules residing on the single- and double-layer graphene mixture.

Dr. W. Xu, H.-K Seo, Prof. T.-W. Lee
Department of Materials Science and Engineering
Pohang University of Science
and Technology (POSTECH)
Pohang, Gyungbuk 790–784, South Korea
E-mail: twlee@postech.ac.kr

Dr. L. Wang, Dr. S. Thomas, Prof. K. S. Kim
Department of Chemistry, School of Natural Science
Center for Superfunctional Materials
Ulsan National Institute of Science and Technology (UNIST)
Ulsan 689–798, South Korea
E-mail: kimks@unist.ac.kr

Y. Liu, Prof. K.-I. Kim
Department of Mathematics
Pohang University of Science and Technology (POSTECH)
Pohang, Gyungbuk 790–784, South Korea

DOI: 10.1002/adma.201405353

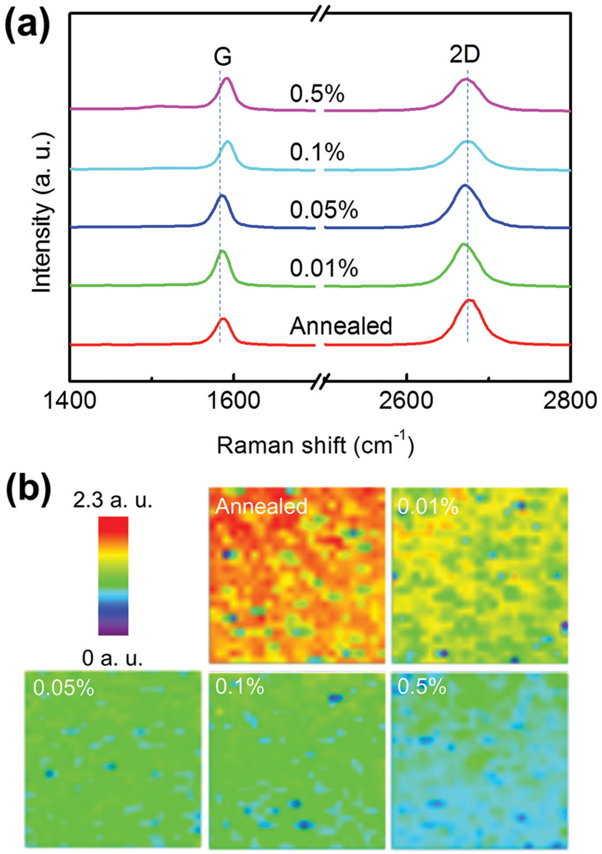

Figure 2. a) Raman spectra of the annealed graphene and the graphene doped with 0.01%, 0.05%, 0.1%, and 0.5% DMC, respectively. b) Mappings of the 2D/G band intensity ratios in a 50 × 50 μm area of the annealed and 0.01%-, 0.05%-, 0.1%-, and 0.5%-DMC-doped graphene.

donating groups that lead to formation of n-doped graphene and carbon nanotubes.[16,17] The intensity ratio I_{2D}/I_G of the 2D and G bands reveals the number of stacked graphene layers.[16] After annealing, our CVD-grown graphene showed an average $I_{2D}/I_G \approx 1.6$, which confirmed that it was a mixture of single layers ($I_{2D}/I_G > 2.3$) and double layers ($I_{2D}/I_G \approx 1$). The color variation in the Raman mapping of the annealed graphene represented different I_{2D}/I_G ratios at different spots, which confirmed the coexistence of the single- (52%) and double-layer (48%) graphene (Supporting Information, SI-2-1). The value of I_{2D}/I_G decreases with the degree of n-type doping,[9] and that of I_{2D}/I_G has a strong dependence on the doping level.[14,18] In the Raman mappings of graphene (Figure 2b) the color change indicated that I_{2D}/I_G decreased as [DMC] increased; this change indicates that n-doping effect increased with [DMC]. The low intensity ratio I_D/I_G (<0.1) of the D and G bands (Supporting Information, SI-2-2) suggests that the graphene sheets contained few defects and that the doping did not cause significant damage.

Two-dimensional potential maps of a 1.2 × 1.2 mm area were recorded using a Kelvin Probe apparatus in air (**Figure 3**a). ϕ decreased as [DMC] increased; this suggests that n-type doping increased with [DMC]. Interestingly, the difference in ϕ from the Kelvin probe tip decreased quasilinearly as log[DMC] increased (Figure 3b). The two-dimensional potential map also shows the uniformity of doping. The fluctuation in ϕ was 0.011, 0.011, 0.065, 0.075, and 0.070 eV for annealed (0%)-, 0.01%-, 0.05%-, 0.1%-, and 0.5%-DMC-doped graphene, respectively. The negligible variations in ϕ imply uniform doping of the surfaces.

Ultraviolet photoelectron spectra (at the secondary electron emission region) of the annealed and doped graphene were compared (Figure 3c). Because the onset of secondary electron emission corresponds to the Fermi level, the doping type and degree can be derived from ϕ, which is calculated as

$$\phi = h\nu - |E_{\mathrm{sec}} - E_F| \tag{1}$$

where $h\nu$ = 21.2 eV (He I source), E_{sec} is the energy at which secondary emission begins, and E_F is the Fermi edge (22.0 eV for the valence band spectrum). The annealed graphene had $\phi = 4.40$ eV, which is quite similar to that of recent reports.[2,19] The graphene doped with 0.01%, 0.05%, 0.1%, and 0.5% DMC solutions had $\phi = 4.3$, 4.0, 3.85, and 3.53 eV, respectively. These values decreased quasilinearly as log[DMC] increased (Figure 3b, black line), in accordance with the Kelvin probe results (Figure 3b, magenta line); this similarity suggests that the doping effect can be controlled by adjusting [DMC] in the solution.

In Equation (1), ϕ is related directly to E_F, but the dopant solution concentration C is related indirectly to E_F via the number of ionized donors N^+. Therefore, the dependence of ϕ on C for n-doped single-layer graphene can be understood through the relationship between C and the dimensionless Fermi level $\varepsilon = E_F/kT$, where k is the Boltzmann constant, and T is the absolute temperature. We obtain (Supporting Information, SI-3) the following relationship

$$N^+(C) = n_i\left[\frac{12}{\pi^2}\xi(\varepsilon) - \frac{\pi^2}{12}\xi^{-1}(\varepsilon)\right] \tag{2}$$

where

$$\xi(\varepsilon) = \int_0^\infty du\,\frac{u}{1+e^{u-\varepsilon}} = \frac{\pi^2}{6} + \frac{\varepsilon^2}{2} + \sum_{j=1}^{\infty}\frac{(-1)^j}{j^2}e^{-j\varepsilon} \tag{3}$$

Here $n_i = \frac{\pi}{6}\left(\frac{kT}{\hbar v_F}\right)^2$ is the intrinsic electron concentration of the undoped graphene at T,[20] C is abbreviation for [DMC], $\hbar$ is the reduced Plank constant, and v_F is the Fermi velocity of graphene charge carriers. u is dimensionless energy $u = E/kT$. $\xi(\varepsilon)$ accounts for the dependence of the doped graphene electron concentration on ε. The asymptotic behavior of $N^+(C)$ varies with ε. i) When $\varepsilon << 1$, i.e., C is relatively low or T is relatively high, $\xi(\varepsilon)$ is roughly an exponential function of ε. This form coincides with that of the semiconductors having an energy gap, which nevertheless holds throughout all regimes. Due to this coincidence, $N^+(C)$ is approximately a linear function of ε in this regime regardless of the energy gap, substituting the Taylor expansion of $\xi(\varepsilon)$ around $\varepsilon = 0$ where $N^+(C) = 0$ into Equation (2). ii) When $\varepsilon >> 1$, i.e., C is relatively high or T is relatively low, $\xi(\varepsilon)$ of the Dirac cone has a parabolic dependence on ε. In turn, Equation (2) determines a parabolic dependence on ε for $N^+(C)$. However, for the gapped dispersion, its exponential

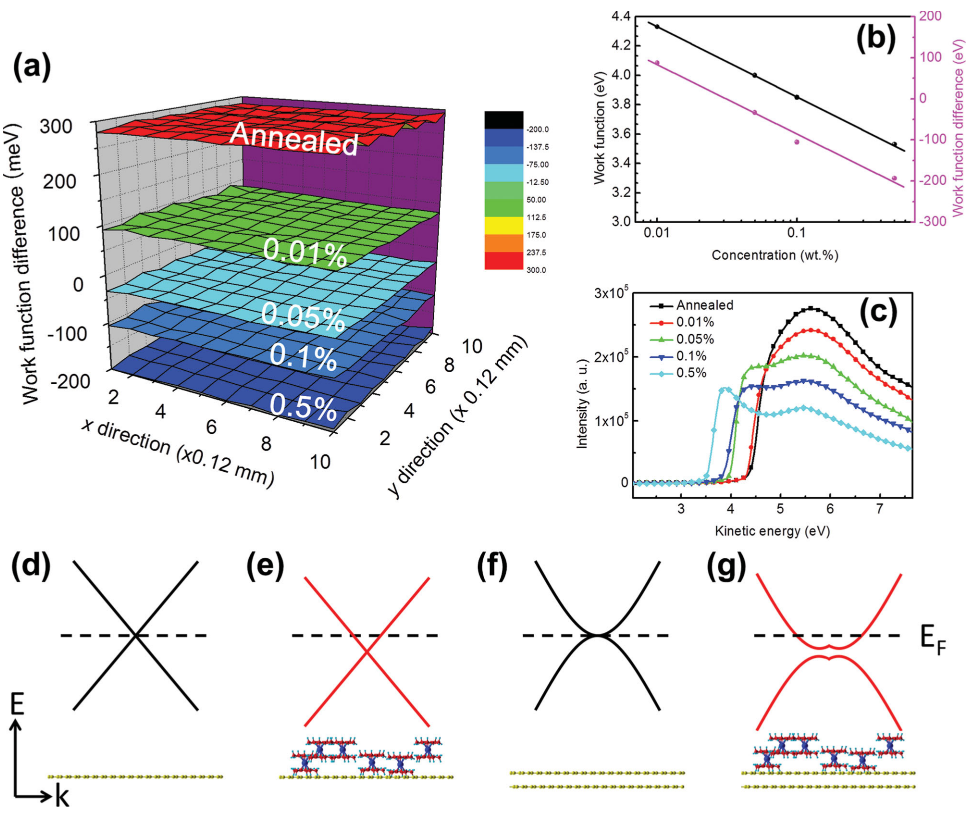

Figure 3. a) Kelvin-probe mapping on a 50 × 50 µm area of the annealed, 0.01%-, 0.05%-, 0.1%-, and 0.5%-DMC-doped graphene, respectively. (b) Work function (from UPS) and the work function difference from the tip (Kelvin probe) versus DMC solution concentration. c) UPS spectra of the annealed, 0.01%-, 0.05%-, 0.1%-, and 0.5%-DMC-doped graphene, respectively. The electronic band structures of (d) undoped and (e) n-doped single-layer fraction, (f) undoped, and (g) n-doped double-layer fraction of the CVD-grown graphene mixture.

dependence on ε for $\xi(\varepsilon)$ results in an exponential dependence on ε for $N^{+}(C)$. (Supporting Information, SI-4 schematically depicts the cause of such asymptotic behaviors of $\xi(\varepsilon)$).

The dependence of $N^{+}(C)$ on ε can be interpreted in terms of C. i) When the donor is at a shallow level, it is ≈100% ionized at room temperature. Therefore, C has the same dependence on ε as $N^{+}(C)$ does. ii) When the donor is at a deep level, which is the case studied in this work, C is equal to an exponential function of ε multiplied by $N^{+}(C)$. Thus, only for gapped dispersion, ϕ has an overall linear dependence on the logarithm of the doping density, log(C), when $\varepsilon >> 1$. Because the experimental ε resides in a crossover regime of 1–32,[21] the obtained quasilinear decrease in ϕ as log[DMC] increases suggests that the energy band gap opened. This opening is most likely induced by doping on the double-layer part of the measured sample,[4,13,22] and implies that the signal from the double-layer graphene dominates in the mixture of single- and double-layer graphene. Furthermore, from the above analysis we propose a criterion to judge whether the donor is at shallow level or at deep level by using the plot of ϕ versus [DMC] in the $\varepsilon \ll 1$ regime: if the plot is linear, the donor is at a shallow level; otherwise, it is at a deep level. The electronic band structures of the single- and double-layer fractions in the graphene mixture before and after doping is depicted (Supporting Information, SI-5). Unlike the single-layer fraction (Figure 3d,e), the undoped double-layer graphene fraction has two touching parabolic bands (Figure 3f). However, the doping on the top layer causes the shift in electrochemical potential between the two layers, which breaks the inversion symmetry of graphene and opens a band gap (Figure 3g).[4]

To examine the doping effect on electrical transport properties, bottom-gate, top-contact GNRFETs were fabricated[23] then n-doped using DMC (**Figure** 4a,b). The parallel e-NWs (Figure 4c) were drawn on a CVD-grown graphene sheet by using our home-built e-nanowire printer[24] to serve as etch masks against the oxygen plasma. Au electrodes were patterned on the e-NWs through a shadow mask. The unprotected region in the graphene sheet was then etched away using oxygen plasma to leave GNRs beneath the e-NWs (Figure 4d).[25] The e-NWs were removed by brief sonication in chloroform. The n-type dopant DMC was then spin-coated on the GNRs.

The transfer and output characteristics were recorded for GNRFETs based on annealed graphene or on graphene doped using [DMC] = 0.01%, 0.05%, 0.1% or 0.5% (Figure 4e and Supporting Information, SI-5). The GNRFET made with annealed GNR showed p-type behavior in air[26] with a positive Dirac point at gate voltage V_G = 38 V, which is consistent with the Raman spectra results and is probably due to adsorbed moisture or oxygen, PMMA residue, or defects introduced during device fabrication.[27,28] In the n-type graphene formed by n-doping with 0.05 wt% DMC solution, the Dirac point shifted negatively to V_G = −25 V. Stronger n-type doping with 0.1 wt%

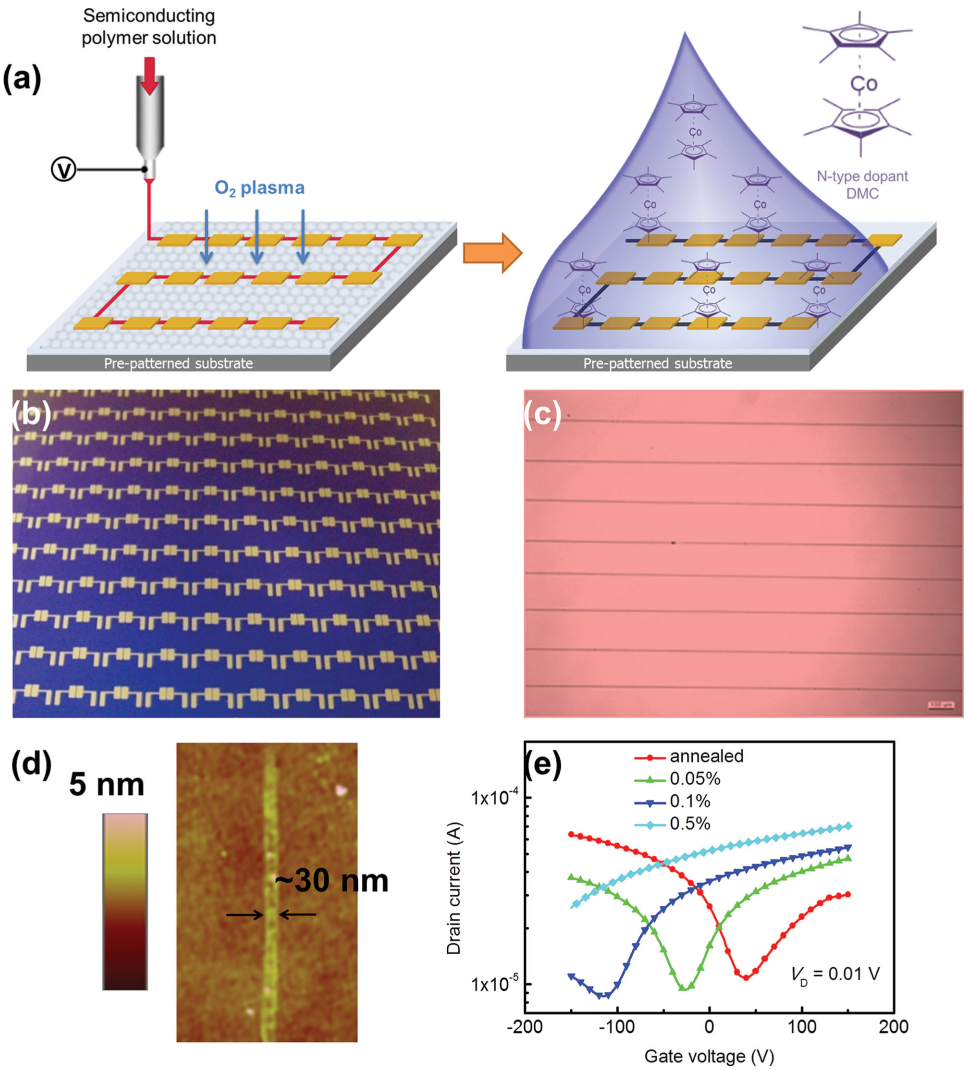

Figure 4. a) Schematic of the fabrication process for a large-scale, n-type-doped GNRFET array, including graphene transfer, e-NW printing, electrode patterning, oxygen plasma treatment, nanowire removal, formation of the final GNRFET array, and spin-coating of the n-type dopant DMC. b) Array of 144 GNRFET devices fabricated on a 4-in. silicon wafer. c) e-NW alignments including parallel lines at pitches of 50 μm. d) AFM image of a typical GNR. e) Typical transfer characteristics of FETs based on annealed and 0.01%-, 0.05%-, 0.1%-, or 0.5%-DMC-doped graphene.

DMC solution further shifted the Dirac point negatively to $V_G = -116$ V. Doping with 0.5 wt% DMC solution shifted the Dirac point out of the tested range of V_G. The strong n-type doping effect confirmed theoretical predictions:[13] the transferred electron charge was tightly localized because of the good adhesion between the aromatic rings in DMC and graphene. This is consistent with the Raman, UPS, and Kelvin probe measurements.

The hole mobility μ_h and electron mobility μ_e of each device were extracted in the linear regions of the transfer curves (Figure 4e).[29] The annealed graphene had $\mu_h = 1450$ cm^2 V^{-1} s^{-1} and $\mu_e = 600$ cm^2 V^{-1} s^{-1}. The 0.05%-DMC-doped GNRFET had a reduced μ_h of ≈940 cm^2 V^{-1} s^{-1} and a significantly increased μ_e of ≈1050 cm^2 V^{-1} s^{-1}. The simultaneous decrease in μ_h and increase in μ_e is consistent with a recent report on chemical transfer n-type doping.[30] We estimate the band gap using the on/off characteristics, $\Delta E_g = E_g - E_g^0 = (2kT/q)\ln(I_{\text{off}}^0/I_{\text{off}})$,[31] where E_g, q, and I_{off} are band gap, electron charge, and off current, respectively. The super note refers to the undoped sample. The estimated band gaps are 7.5 and 11.6 meV for 0.05% and 0.1% DMC doped samples.

In summary, we provide experimental evidence and theoretical discussions to reveal the doping effect of DMC on a CVD-grown single- and double-layer graphene mixture. The strong n-type doping shifted the Dirac point substantially in the negative direction and reduced the ϕ of graphene. ϕ decreased quasilinearly as log[DMC] increased; this relationship could be very useful in tuning the electrical properties of graphene. A possible role of single- and double-layer fractions in the overall characteristics of the CVD-grown graphene suggests band gap opening as the cause of the established relationship. This suggests that the double-layer fraction had a dominant influence on the Fermi level of our CVD-grown graphene. Scalable site- and alignment-controlled graphene nanoribbons doped with the solution-processed dopant DMC were produced on a wafer scale using e-NW lithography. μ_e of 1050 cm^2 V^{-1} s^{-1} was obtained for a 0.05%-DMC-doped GNRFET. We envision that the doping approach and the established local-quasilinear relationship have significance on the broad application of CVD-grown graphene in future nanoelectronics.

Supporting Information

Supporting Information is available from the Wiley Online Library or from the author.

Acknowledgements

W.X. and L.W. contributed equally to this work. This research was supported by the MSIP (Ministry of Science, ICT, and Future Planning), Korea, under the "IT Consilience Creative Program" (NIPA-2014-H0201–14–1001) supervised by the NIPA (National IT Industry Promotion Agency). This work was also supported by the Basic Research Program through the National Research Foundation (NRF) of Korea, funded by the Ministry of Education (NRF-2013R1A1A2012660 and National honor scientist program: 2010–0020414). Note: The text on line 20 of the left column on page 1621 was corrected on March 2, 2015 after initial publication online.

Received: November 23, 2014
Published online: January 21, 2015

---

[1] a) K. S. Novoselov, A. K. Geim, S. V. Morozov, D. Jiang, Y. Zhang, S. V. Dubonos, I. V. Grigorieva, A. A. Firsov, *Science* **2004**, *306*, 666; b) F. Schwierz, *Nature* **2011**, *472*, 41; c) L. Ma, J. Wang, F. Ding, *ChemPhysChem* **2013**, *14*, 47; d) S.-J. Byun, H. Lim, G.-Y. Shin, T.-H. Han, S. H. Oh, J.-H. Ahn, H. C. Choi, T.-W. Lee, *J. Phys. Chem. Lett.* **2011**, *2*, 493; e) Z. Yan, J. Lin, Z. Peng, Z. Sun, Y. Zhu, L. Li, C. Xiang, E. L. Samuel, C. Kittrell, J. M. Tour, *ACS Nano* **2012**, *6*, 9110; f) K. S. Kim, Y. Zhao, H. Jang, S. Y. Lee, J. M. Kim, K. S. Kim, J.-H. Ahn, P. Kim, J.-Y. Choi, B. H. Hong, *Nature* **2009**, *457*, 706; g) H. Kim, E. Kim, W.-J. Lee, J. Jung, *Electron. Mater. Lett.* **2013**, *9*, 417; h) M. Kim, H. An, W.-J. Lee, J. Jung, *Electron. Mater. Lett.* **2013**, *9*, 517.

[2] a) T.-H. Han, Y. Lee, M.-R. Choi, S.-H. Woo, S.-H. Bae, B. H. Hong, J.-H. Ahn, T.-W. Lee, *Nat. Photonics* **2012**, *6*, 105; b) S. Bae, H. Kim, Y. Lee, X. Xu, J.-S. Park, Y. Zheng, J. Balakrishnan, T. Lei, H. R. Kim, Y. I. Song, Y.-J. Kim, K. S. Kim, B. Özyilmaz, J.-H. Ahn, B. H. Hong, S. Iijima, *Nat. Nanotechnol.* **2010**, *5*, 574.

[3] H. Liu, Y. Liu, D. Zhu, *J. Mater. Chem.* **2011**, *21*, 3335.

[4] J. Park, S. B. Jo, Y.-J. Yu, Y. Kim, J. W. Yang, W. H. Lee, H. H. Kim, B. H. Hong, P. Kim, K. Cho, K. S. Kim, *Adv. Mater.* **2012**, *24*, 407.

[5] I.-Y. Lee, H.-Y. Park, J.-H. Park, J. Lee, W.-S. Jung, H.-Y. Yu, S.-W. Kim, G.-H. Kim, J.-H. Park, *Org. Electron.* **2013**, *14*, 1586.

[6] X. Wang, X. Li, L. Zhang, Y. Yoon, P. K. Weber, H. Wang, J. Guo, H. Dai, *Science* **2009**, *324*, 768.

[7] a) H. Wang, T. Maiyalagan, X. Wang, *ACS Catal.* **2012**, *2*, 781; b) B. Guo, L. FangB. Zhang, J. R. Gong, *Insci. J.* **2011**, *1*, 80; c) B. Guo, Q. Liu, E. Chen, H. Zhu, L. Fang, J. R. Gong, *Nano Lett.* **2010**, *10*, 4975; d) A. C. Ferrari, J. C. Meyer, V. Scardaci, C. Casiraghi, M. Lazzeri, F. Mauri, S. Jiang, D. Piscanec, K. S. Novoselov, S. Roth, A. K. Gein, *Phys. Rev. Lett.* **2006**, *97*, 187401; e) U. N. Maiti, W. J. Lee, J. M. Lee, Y. Oh, J. Y. Kim, J. E. Kim, J. Shim, T. H. Han, S. O. Kim, *Adv. Mater.* **2014**, *26*, 40; f) J. M. Yun, S. Park, Y. H. Hwang, E.-S. Lee, U. Maiti, H. Moon, B.-H. Kim, B.-S. Bae, Y.-H. Kim, S. O. Kim, *ACS Nano* **2014**, *8*, 650; g) J. O. Hwang, J. S. Park, D. S. Choi, J. Y. Kim, S. H. Lee, K. E. Lee, Y.-H. Kim, M. H. Song, S. Yoo, S. O. Kim, *ACS Nano* **2012**, *6*, 159.

[8] a) X. Li, W. Cai, L. Colombo, R. S. Ruoff, *Nano Lett.* **2009**, *9*, 4268; b) I. Vlassiouk, M. Regmi, P. Fulvio, S. Dai, P. Datskos, G. Eres, S. Smirnov, *ACS Nano* **2013**, *7*, 2790; c) J. K. Wassei, M. Mecklenburg, J. A. Torres, J. D. Fowler, B. C. Regan, R. B. Kaner, B. H. Weiller, *Small* **2012**, *8*, 1415.

[9] P. Wei, N. Liu, H. R. Lee, E. Adijanto, L. Ci, B. D. Naab, J. Q. Zhong, J. Park, W. Chen, Y. Cui, Z. Bao, *Nano Lett.* **2013**, *13*, 1890.

[10] A. N. Sokolov, F. L. Yap, N. Liu, K. Kim, L. Ci, O. B. Johnson, H. Wang, M. Vosgueritchian, A. L. Koh, J. Chen, J. Park, Z. Bao, *Nat. Commun.* **2013**, *4*, 2402.

[11] C. K. Chan, W. Zhao, S. Barlow, S. Marder, A. Kahn, *Org. Electron.* **2008**, *9*, 575.

[12] C. V. Chan, A. Kahn, *Appl. Phys. A.* **2009**, *95*, 7.

[13] A. J. Samuels, J. D. Carey, *ACS Nano* **2013**, *7*, 2790.

[14] A. Das, S. Pisana, B. Chakraborty, S. Piscanec, S. K. Saha, U. V. Waghmare, K. S. Novoselov, H. R. Krishnamurthy, A. K. Geim, A. C. Ferrari, A. K. Sood, *Nat. Nanotechnol.* **2008**, *3*, 210.

[15] A. C. Farrari, D. M. Basko, *Nat. Nanotechnol.* **2013**, *8*, 235.

[16] X. Dong, D. Fu, W. Fang, Y. Shi, P. Chen, L.-J. Li, *Small* **2009**, *5*, 1422.

[17] a) H.-J. Shin, S. M. Kim, S.-M. Yoon, A. Benayad, K. K. Kim, S. J. Kim, H. K. Park, J.-Y. Choi, Y. H. Lee, *J. Am. Chem. Soc.* **2008**, *130*, 2062; b) R. Voggu, C. S. Rout, A. D. Franklin, T. S. Fisher, C. N. R. Rao, *J. Phys. Chem. C* **2008**, *112*, 13053.

[18] S. Pisana, M. Lazzeri, C. Casiraghi, K. S. Novoselov, A. K. Geim, A. C. Ferrari, F. Mauri, *Nat. Mater.* **2007**, *6*, 198.

[19] J. Park, W. H. Lee, S. Huh, S. H. Sim, S. B. Kim, K. Cho, B. H. Hong, K. S. Kim, *J. Phys. Chem. Lett.* **2011**, *2*, 841.

[20] T. Fang, A. Konar, H. Xing, D. Jena, *App. Phys. Lett.* **2007**, *91*, 092109.

[21] E_F or ε was obtained by offsetting ϕ with that of the concentration corresponding to the zero gate voltage in Figure 4e.

[22] A. H. Castro Neto, F. Guinea, N. M. R. Peres, K. S. Novoselov, A. K. Geim, *Rev. Mod. Phys.* **2009**, *81*, 109.

[23] a) B. J. Kim, S.-K. Lee, M. S. Kang, J.-H. Ahn, J. H. Cho, *ACS Nano* **2012**, *6*, 8646; b) S.-K. Lee, B. J. Kim, H. Jang, S. C. Yoon, C. Lee, B. H. Hong, J. A. Rogers, J. H. Cho, J.-H. Ahn, *Nano Lett.* **2011**, *11*, 4642; c) J. M. Yun, S. Park, Y. H. Hwang, E.-S. Lee, U. Maiti, H. Moon, B.-H. Kim, B.-S. Bae, Y.-H. Kim, S. O. Kim, *ACS Nano* **2014**, *8*, 650; d) S.-Y. Chen, P.-H. Ho, R.-J. Shiue, C.-W. Chen, W.-H. Wang, *Nano Lett.* **2012**, *12*, 964; e) J. Lee, L. Tao, K. N. Parrish, Y. Hao, R. S. Ruoff, D. Akinwande, *Appl. Phys. Lett.* **2012**, *101*, 252109; f) A. Reina, X. Jia, J. Ho, D. Nezich, H. Son, V. Bulovic, M. S. Dresselhaus, J. Kong, *Nano Lett.* **2009**, *9*, 30.

[24] S.-Y. Min, T.-S. Kim, B. J. Kim, H. Cho, Y.-Y. Noh, H. Yang, J. H. Cho, T.-W. Lee, *Nat. Commun.* **2013**, *4*, 1773.

[25] a) W. Xu, T.-S. Lim, H.-K. Seo, S.-Y. Min, H. Cho, M.-H. Park, Y.-H. Kim, T.-W. Lee, *Small* **2014**, *10*, 1999; b) W. Xu, H.-K. Seo, S.-Y. Min, H. Cho, T.-S. Lim, C.-y. Oh, Y. Lee, T.-W. Lee,*Adv. Mater.* **2014**, *26*, 3459.

[26] a) Z. Cheng, Q. Zhou, C. Wang, Q. Li, C. Wang, Y. Fang, *Nano Lett.* **2011**, *11*, 767; b) Y.-C. Lin, C.-C. Lu, C.-H. Yeh, C. Jin, K. Suenaga, P.-W. Chiu, *Nano Lett.* **2012**, *12*, 414; c) F. Schedin, A. K. Geim, S. V. Morozov, E. W. Hill, P. Blake, M. I. Katsnelson, K. S. Novoselov, *Nat. Mater.* **2007**, *6*, 652.

[27] A. Pirkle, J. Chan, A. Venugopal, D. Hinojos, C. W. Magnuson, S. McDonnell, L. Colombo, E. M. Vogel, R. S. Ruoff, R. M. Wallace, *Appl. Phys. Lett.* **2011**, *99*, 122108.

[28] J. W. Suk, W. H. Lee, J. Lee, H. Chou, R. D. Piner, Y. Hao, D. Akinwande, R. S. Ruoff, *Nano Lett.* **2013**, *13*, 1462.

[29] a) F. Schwierz, *Nat. Nanotechnol.* **2010**, *5*, 487; b) I. Martin-Fernandez, D. Wang, Y. Zhang, *Nano Lett.* **2012**, *12*, 6175.

[30] S. Some, J. Kim, L. Lee, A. Kulkarni, Y. Yoon, S. M. Lee, T. Kim, H. Lee, *Adv. Mater.* **2012**, *24*, 5481.

[31] a) F. N. Xia, D. B. Farmer, Y. M. Lin, P. Avouris, *Nano. Lett.* **2010**, *10*, 715; b) W. Zhang, C.-T. Lin, K.-K. Liu, T. Tite, C.-Y. Su, C.-H. Chang, Y.-H. Lee, C.-W. Chu, K.-H. Wei, J.-L. Kuo, L.-J. Li, *ACS Nano* **2011**, *5*, 7517.